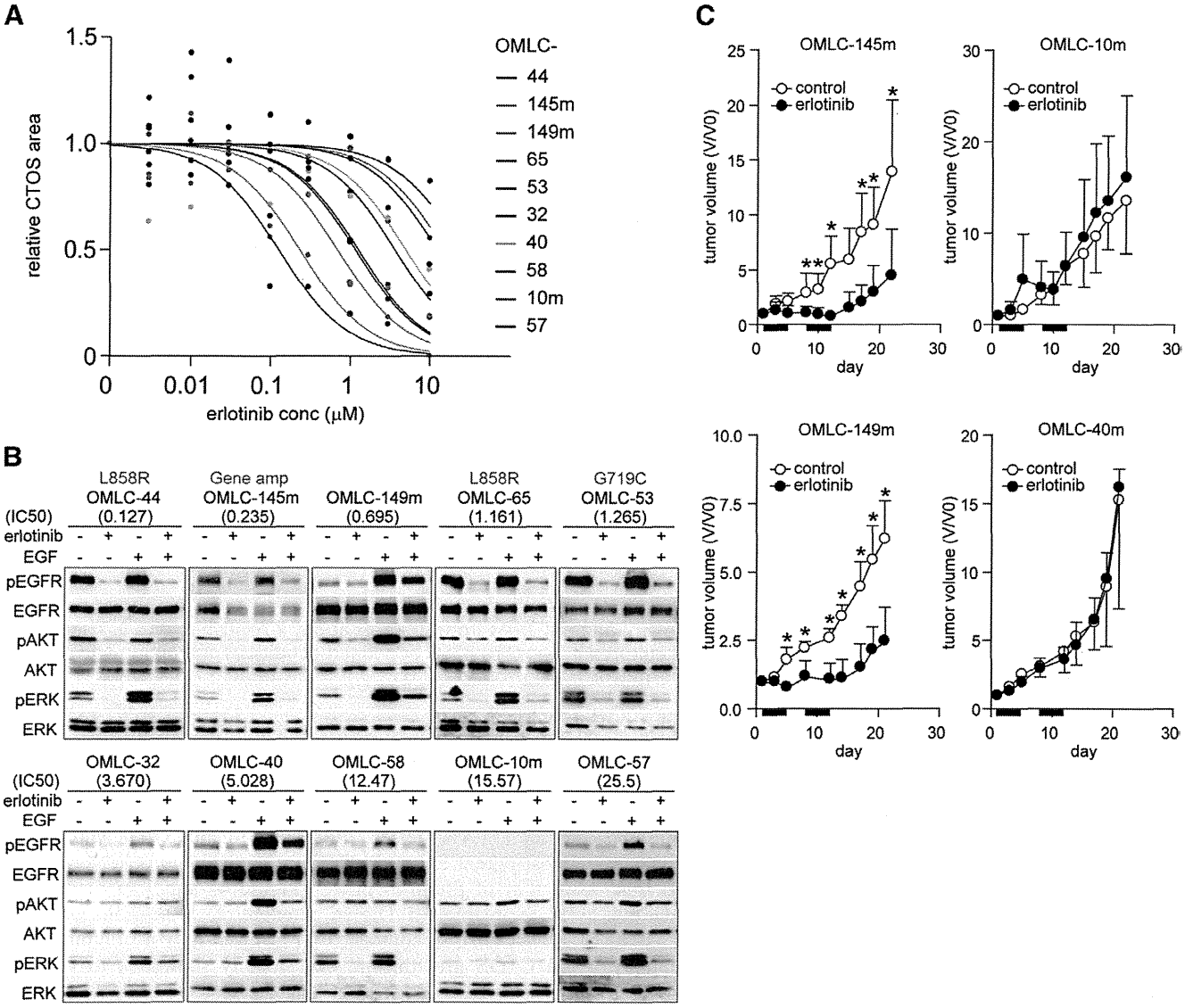

FIGURE 3. Effect of erlotinib on CTOS growth and signal transduction. *A*, In vitro dose–response curve of erlotinib sensitivity with 10 clinical cases. Origins of the cases are indicated in ascending order of IC50. *B*, Western blot of EGFR signaling pathway from 10 clinical cases, in ascending order of IC50. CTOSs were cultured under growth-factor–starved conditions and pulsed for 15 minutes with 10ng/ml EGF in the presence or absence of 1 μM erlotinib. *C*, Effects of erlotinib on the growth of xenograft tumors derived from OMLC-145 (EGFR overexpresser), OMLC-10 (EGFR-nonexpresser), OMLC-149 (*EGFR* wt), and OMLC-40 (*EGFR* wt). The CTOSs were transplanted in NOD/SCID mice ($n = 5$). Erlotinib was administered orally once a day ×5 for 2 weeks, indicated as black bars. Tumor volume at each time point (V) was corrected by that on day 1 (V0). Open circles, vehicle-treated controls; closed circles, erlotinib-treated groups. IC50, inhibitory concentration. *$p < 0.05$

The EGFR TKIs gefitinib and erlotinib are known to be effective against lung cancer harboring active *EGFR* mutations[1,19] or EGFR gene amplification.[20,21] We examined whether the response of CTOSs to EGFR TKI was consistent with these clinical findings, and found that erlotinib sensitivity varied among individual patients (Fig. 3A). Three EGFR active mutant cases and one gene amplification case were among the top five most sensitive cases (Supplementary Fig. 5A and B, Supplemental Digital Content 6, http://links.lww.com/JTO/A360). One advantage of analyzing CTOSs is the ability to assess the status of intracellular signaling and the change of status after drug treatment in individual patient samples. We subjected the CTOSs to immunoblot analysis to investigate the effect of erlotinib on intracellular signaling. *EGFR* mutants (OMLC-44, OMLC-53, and OMLC-65) and the *EGFR* overexpresser (OMLC-145) showed high levels of phosphorylation of EGFR and AKT, even under growth-factor–starved conditions, indicating constitutive activation of EGFR signaling (Fig. 3B). In these cases, the phosphorylation of EGFR, AKT, and extracellular signal-regulated kinase, was

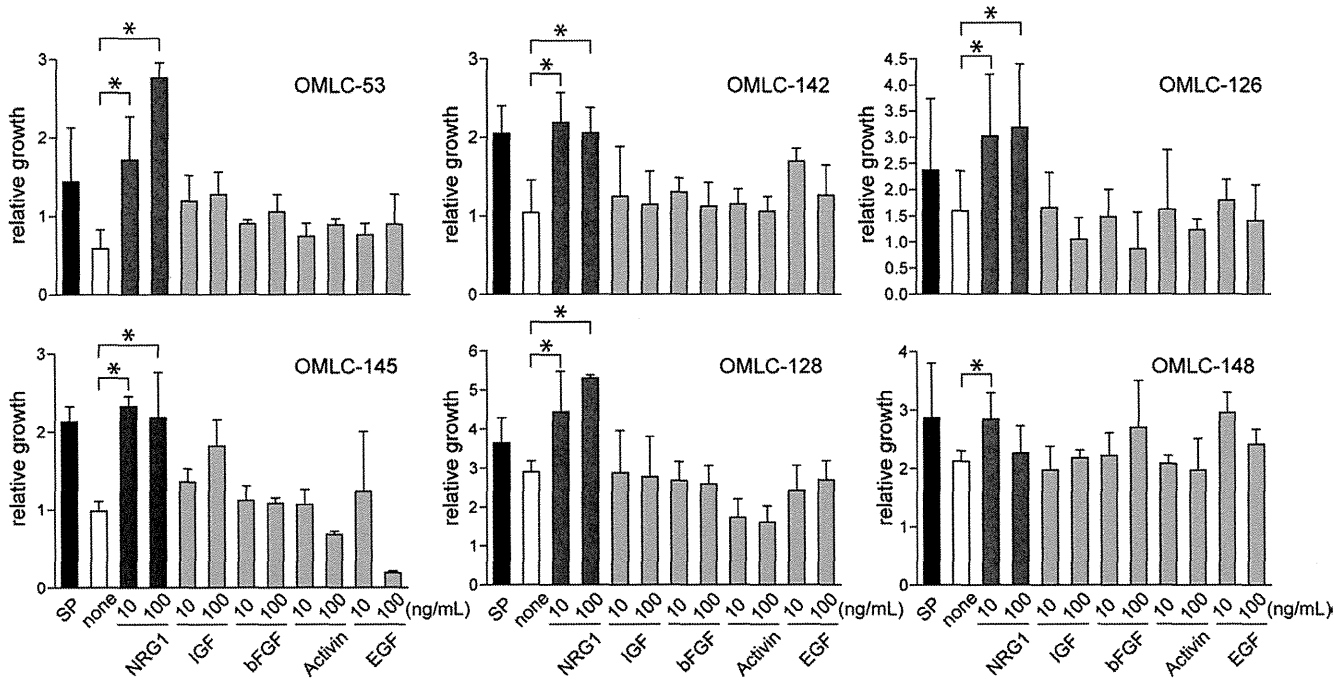

FIGURE 4. NRG1stimulated CTOS growth in vitro. Growth ratio of CTOSs from six cases at day 7 relative to day 0. The CTOSs were embedded in Matrigel growth factor reduced and cultured in StemPro hESC or defined conditions containing NRG1, Long-IGF (IGF), bFGF, Activin A (Activin), or EGF at 10 ng/mlL or 100 ng/ml. *$p < 0.05$.

diminished after erlotinib treatment, even in the presence of the EGFR ligand EGF.

One case of CTOS (OMLC-149), in which we could detect neither known *EGFR* mutations nor EGFR gene amplification, showed high sensitivity to erlotinib and gefitinib, whereas other CTOSs with wild-type *EGFR* were resistant to erlotinib (Fig. 3A, Supplementary Fig. 5C and D). The phosphorylation of EGFR under starved conditions was not high; however, in contrast with other *EGFR* wild-type cases, the phosphorylation of both AKT and ERK was substantially high, which was suppressed by erlotinib treatment.

Next, we assessed whether the results of the CTOS sensitivity assay or the signal analysis in vitro reflected the sensitivity to erlotinib in vivo using the following four CTOSs: OMLC-145 (erlotinib sensitive, EGFR gene amplification), OMLC-10 (erlotinib resistant, EGFR not expressed), OMLC-149 (erlotinib sensitive, *EGFR* wild-type), and OMLC-40 (erlotinib resistant, *EGFR* wild-type). We transplanted these CTOSs into the flanks of NOD/SCID mice. Consistent with the results of the in vitro experiments, growth of the tumors derived from erlotinib-sensitive CTOSs was suppressed by erlotinib treatment, whereas no effect was observed in the tumors derived from erlotinib-resistant CTOSs (Fig. 3C). Thus, the results of the in vitro CTOS sensitivity assay and signal transduction assay with an EGFR inhibitor were in parallel with the therapeutic efficacy in vivo in the four examined cases.

Neuregulin 1 Stimulated CTOS Growth In Vitro

To determine which growth factors contributed to the CTOS growth in culture, we performed an assay in which the growth factors NRG1/heregulinβ1, insulin-like growth factor (IGF), basic fibroblast growth factor (bFGF), activin A, and epidermal growth factor (EGF), in StemPro hESC[22] were added one at a time to the basal medium. In 10 of 13 cases (71.4%) tested, the HER3 ligand NRG1 showed the most potent effect on CTOS growth at the dose compatible to that of StemPro hESC (Figure 4, Supplementary Table 1, Supplemental Digital Content 2, http://links.lww.com/JTO/A356). In contrast, EGF showed only a minimal effect on CTOS growth, and occasionally showed a toxic effect (Fig. 4; OMLC-145). Among the tested cases, two CTOSs from squamous cell carcinoma did not respond to NRG1 (Supplementary Table 1, Supplemental Digital Content 2, http://links.lww.com/JTO/A356).

Analysis of intracellular signaling revealed that NRG1 was the most potent inducer of AKT phosphorylation (Fig. 5A). Next, we analyzed the localization of HER3 phosphorylation by NRG1 in CTOSs by immunohistochemistry (Fig. 5B). Phosphorylation of HER3 and AKT was detected after NRG1 stimulation. As demonstrated by ZO-1/E-cadherin and EGFR staining, the CTOSs from OMLC-53 had polarity, in which the apical side was outside of CTOSs (Fig. 5B). HER3 phosphorylation was detected at the basolateral membrane of the cells in the CTOS. However, CTOSs from OMLC-128 did not show clear polarity.

We then challenged the CTOSs cultured in NRG1-containing medium or StemPro hESC with a neutralizing antibody against HER3.[23] The growth (Fig. 5C) and the phosphorylation of HER3 and AKT (Fig. 5D) were partially suppressed by the antibody. Taken together, our findings show

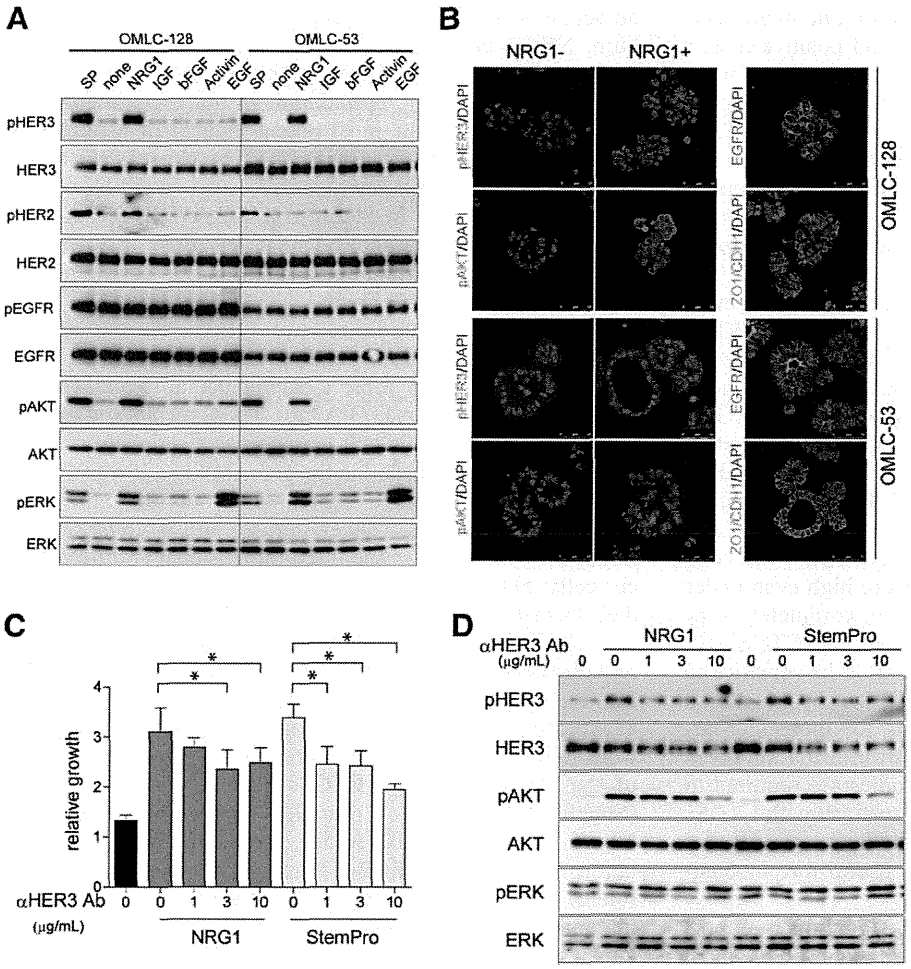

FIGURE 5. Effect of NRG1 on pathway activation in CTOSs. *A*, Western blot for ErbB family signaling pathway of OMLC-128 and OMLC-53. CTOSs were cultured under growth-factor–starved conditions and stimulated by 10 ng/ml of each indicated growth factor for 15 minutes. *B*, Immunohistochemistry of phospho-HER3 and phospho-AKT after NRG1 stimulation. OMLC-128 or OMLC-53 CTOSs were cultured under starvation conditions and stimulated by 10 ng/ml NRG1 for 6 hours (pHER3) or 1 hour (pAKT). EGFR, ZO1, and E-cadherin staining indicate the polarity of the CTOSs. *C*, Inhibitory effect of anti-HER3 antibody on growth of OMLC-128 CTOSs. CTOSs were embedded in Matrigel growth factor reduced, cultured in basal medium containing 10 ng/ml NRG1 or StemPro hESC, and treated with the indicated doses of anti-HER3 antibody. $*p < 0.05$. *D*, Effect of anti-HER3 antibody on signal transduction of OMLC-128. CTOSs were cultured in StemPro containing the indicated dose of anti-HER3 antibody for 24 hours. StemPro hESC; IGF; long-IGF1, Activin; Activin A.

that NGR1/HER3 signaling played a role in the culture of lung CTOSs.

DISCUSSION

Primary culture of lung cancer cells has been attempted for decades, using two basic approaches: histoculture and dissociation-based culture. In histoculture, tumors are cultured directly[24,25] or on gel matrices after being minced into small pieces.[26–28] In dissociation-based culture, tumors are enzymatically dissociated into single cells or cell aggregates of several cells; then the cells or cell aggregates are cultured on the dish[29] or in gel matrices.[30,31] In these methods, the cultured cells are mixtures of tumor cells and host cells in varying degrees. In contrast, CTOS technology enables us to culture mostly purified lung cancer cells as spheroids in a medium with defined growth factors, and allows us to obtain reproducible results; these features are essential for bioassays, such as treatment sensitivity assays and pathway-activation assays.

The success rate of preparing CTOSs from lung cancer was 80.0%, which is relatively low compared with the high success rate (98.7%) achieved with colorectal cancer.[16] This difference may be partly because of the relatively poor content of cancer cells in the lung cancer samples. In addition, as lung cancer tissues contain more fibrous component than colorectal cancer tissues do, optimizing the protocol of tissue dissociation might improve the CTOS preparation from tiny biopsy samples of lung cancer. The success rate of tumor formation with lung cancer CTOSs in NOD-scid mice was also relatively low, 33.3%, compared with the results with colorectal cancer.[16] Compared with colorectal cancer, lung cancer cell growth might be more dependent on the cancer-associated microenvironment, which might not be replicated in mouse subcutaneous tissue.

CSC theory has been recently proposed and widely investigated; this theory states that only a minor population of cancer cells has the capacity of self-renewal and multipotency of differentiation; therefore, cancers form with a hierarchy dominated by the CSCs.[18,32] CTOSs share some characteristics of CSCs, including sphere-forming capacity in suspension culture with serum-free medium, and tumorigenic capacity in immunodeficient mice. However, CTOSs and CSC-derived spheroids are different in several aspects. First, lung CSCs are reportedly CD133-positive cells, which are rare in tumors and enriched in CSC-derived spheroids,[18] whereas the level of CD133-positive cells was not enriched in CTOSs (Supplementary Fig. 3, Supplemental Digital Content 4, http://links.lww.com/JTO/A358). Second, the expression levels of

differentiation markers, including cytokeratin and neural cell adhesion marker, are reportedly low in CD133-positive cells,[18] whereas the expression levels of these markers in CTOSs were similar to those in the original tumors (Supplementary Fig. 2, Supplemental Digital Content 3, http://links.lww.com/JTO/A357). Thus, the cells comprising the CTOS represented the major population of cancer cells within the patient's tumor, and are not likely derived from a minority cell population in the tumor, although our experiments do not exclude the existence of CSCs in CTOSs.

We showed that the CTOS method can be used to evaluate EGFR signaling and the response to an EGFR TKI in primary cultured lung cancer cells from individual patients. Tumors harboring EGFR-activating mutations and gene amplification are known to be clinically sensitive to EGFR TKIs,[1–3,20,21] and correspondingly, these cases were sensitive to erlotinib in the CTOS assay in vitro (Fig. 3A). In terms of intracellular signaling, the levels of AKT phosphorylation are reportedly high in EGFR TKI–sensitive patients or cell lines.[21,33] Indeed, in the erlotinib-sensitive CTOSs, the rates of phosphorylation of EGFR and AKT were high even under growth-factor–starved conditions, and were completely suppressed by erlotinib treatment. We also found one CTOS with wild-type *EGFR* and no gene amplification to be sensitive to erlotinib in vitro and in vivo. Thus, CTOS might provide an alternative method for selecting patients for molecular-targeted drugs, in addition to the *snapshot* of information given by assessing biopsy samples. Further studies are required to test the relationship between the sensitivity assay with CTOSs and the patients' clinical response to specific treatments and determine whether the CTOS method is useful for personalized medicine.

We found here that NRG1-HER3 signaling is important for CTOS culture from NSCLC. NRG1 showed the most potent effect on CTOS growth in 71.4% cases at the tested doses, yet other growth factors also promoted CTOS growth to some extent (Fig. 4). In some cases, the growth-promoting effect of NRG1 was saturated at 10 ng/ml. This might be because of the internalization and degradation of HER3 after ligand binding. HER3 is a member of ErbB family of transmembrane tyrosine kinase receptors. HER3 lacks tyrosine kinase activity, and transduces downstream signals by forming heterodimers with other tyrosine kinase receptors.[9] As HER3 has six docking sites for phosphatatidylinositol-3 kinase (PIK3) p85, it can potently activate the PI3K-AKT pathway.[34] Among the growth factors examined in this study, NRG1 most strongly induced AKT phosphorylation in CTOSs (Fig. 5A). Despite the growth-promoting effect of NRG1 on the CTOSs, we only observed a marginal inhibitory effect of the anti-HER3 antibody (Fig 5D). This might be because of the antibody's ability to block signaling; it is also possible that the tight junctions in CTOSs (illustrated by ZO-1 staining in Fig. 5B) stopped the antibody from penetrating sufficiently.

The NRG1-HER3 pathway plays important roles in the maintenance of normal airway epithelium.[35] HER3 and its ligands are both constitutively expressed in normal lung alveolar cells. NRG1 is secreted to the apical side, whereas HER3 is expressed in the basolateral side; thus, HER3 has no access to the ligands. Upon injury to the alveolar epithelium, NRG1 binds to HER3 and the signal contributes to wound healing. Lung cancer might use the wound healing system of normal lung epithelium. In our experiments with CTOSs, NRG1 was the most potent inducer of proliferation and AKT phosphorylation (Fig. 5A). The phosphorylation of HER3 after NRG1 treatment was observed on the basolateral membrane (Fig. 5B). In StemPro hESC, CTOSs from squamous cell carcinomas showed relatively poor growth compared with CTOSs from adenocarcinomas (Supplementary Fig. 4B, Supplemental Digital Content 5, http://links.lww.com/JTO/A359). In addition, two CTOSs from squamous cell carcinomas did not depend on any of the growth factors tested (Supplementary Table 1, Supplemental Digital Content 2, http://links.lww.com/JTO/A356). These results suggest that CTOSs from squamous cell carcinomas require growth factors other than those tested in the present study. It was recently reported that NRG1-HER3 signaling promotes mammosphere formation from breast cancer–derived single cells.[36] NRG1 might exert an effect on the three-dimensional culture of cancer cells; although in CTOSs, NRG1 was not necessary for their formation.

It is reported that activation of PI3K-AKT by EGFR requires HER3, using gefitinib-sensitive cell lines.[37] NRG1 is also reported to promote tumor growth in two of eight lung adenocarcinoma cell lines (25%), and both of the responders were *EGFR* mutants.[38] However, in the present study, some of the *EGFR* wild-type CTOSs also responded to NRG1 (Supplementary Table 1, Supplemental Digital Content 2, http://links.lww.com/JTO/A356), probably via phosphorylation of HER3 by HER2. These results suggested that the role of HER3 signaling might not be restricted to the *EGFR* mutants. Further studies are required to assess whether NRG1 alone can be substituted for StemPro hESC and allow not only growth, but also maintenance of original characters, and tumorigenicity of CTOSs.

In conclusion, the present findings show that the novel CTOS method can be successfully used to obtain primary lung tumor cells of high viability and purity. Thus, it is possible that CTOSs could be a new platform for studying lung cancer biology, and for examining an individual patient's response to clinical treatment.

ACKNOWLEDGMENTS

This work was supported in part by KAKENHI (22791240), the Charitable Trust Osaka Cancer Researcher-Found (HE), and the Japan Advanced Molecular Imaging Program (J-AMP) of the Ministry of Education, Culture, Sports, Science, and Technology of Japan (MI).

We thank M. Ito and T. Yasuda for technical assistance, and M. Izutsu for secretarial assistance.

REFERENCES

1. Lynch TJ, Bell DW, Sordella R, et al. Activating mutations in the epidermal growth factor receptor underlying responsiveness of non-small-cell lung cancer to gefitinib. *N Engl J Med* 2004;350:2129–2139.
2. Zhou C, Wu YL, Chen G, et al. Erlotinib versus chemotherapy as first-line treatment for patients with advanced EGFR mutation-positive

non-small-cell lung cancer (OPTIMAL, CTONG-0802): a multicentre, open-label, randomised, phase 3 study. *Lancet Oncol* 2011;12:735–742.
3. Kobayashi S, Boggon TJ, Dayaram T, et al. EGFR mutation and resistance of non-small-cell lung cancer to gefitinib. *N Engl J Med* 2005;352:786–792.
4. Bean J, Brennan C, Shih JY, et al. MET amplification occurs with or without T790M mutations in EGFR mutant lung tumors with acquired resistance to gefitinib or erlotinib. *Proc Natl Acad Sci USA* 2007;104:20932–20937.
5. Kosaka T, Yatabe Y, Endoh H, et al. Analysis of epidermal growth factor receptor gene mutation in patients with non-small cell lung cancer and acquired resistance to gefitinib. *Clin Cancer Res* 2006;12:5764–5769.
6. Engelman JA, Zejnullahu K, Mitsudomi T, et al. MET amplification leads to gefitinib resistance in lung cancer by activating ERBB3 signaling. *Science* 2007;316:1039–1043.
7. Cappuzzo F, Toschi L, Tallini G, et al. Insulin-like growth factor receptor 1 (IGFR-1) is significantly associated with longer survival in non-small-cell lung cancer patients treated with gefitinib. *Ann Oncol* 2006;17:1120–1127.
8. Wheeler DL, Dunn EF, Harari PM. Understanding resistance to EGFR inhibitors-impact on future treatment strategies. *Nat Rev Clin Oncol* 2010;7:493–507.
9. Baselga J, Swain SM. Novel anticancer targets: revisiting ERBB2 and discovering ERBB3. *Nat Rev Cancer* 2009;9:463–475.
10. Shigematsu H, Takahashi T, Nomura M, et al. Somatic mutations of the HER2 kinase domain in lung adenocarcinomas. *Cancer Res* 2005;65:1642–1646.
11. Buttitta F, Barassi F, Fresu G, et al. Mutational analysis of the HER2 gene in lung tumors from Caucasian patients: mutations are mainly present in adenocarcinomas with bronchioloalveolar features. *Int J Cancer* 2006;119:2586–2591.
12. Zhou BB, Peyton M, He B, et al. Targeting ADAM-mediated ligand cleavage to inhibit HER3 and EGFR pathways in non-small cell lung cancer. *Cancer Cell* 2006;10:39–50.
13. Shoemaker RH. The NCI60 human tumour cell line anticancer drug screen. *Nat Rev Cancer* 2006;6:813–823.
14. Tsuji K, Kawauchi S, Saito S, et al. Breast cancer cell lines carry cell line-specific genomic alterations that are distinct from aberrations in breast cancer tissues: comparison of the CGH profiles between cancer cell lines and primary cancer tissues. *BMC Cancer* 2010;10:15.
15. Daniel VC, Marchionni L, Hierman JS, et al. A primary xenograft model of small-cell lung cancer reveals irreversible changes in gene expression imposed by culture in vitro. *Cancer Res* 2009;69:3364–3373.
16. Kondo J, Endo H, Okuyama H, et al. Retaining cell-cell contact enables preparation and culture of spheroids composed of pure primary cancer cells from colorectal cancer. *Proc Natl Acad Sci USA* 2011;108:6235–6240.
17. Endo H, Murata K, Mukai M, Ishikawa O, Inoue M. Activation of insulin-like growth factor signaling induces apoptotic cell death under prolonged hypoxia by enhancing endoplasmic reticulum stress response. *Cancer Res* 2007;67:8095–8103.
18. Eramo A, Lotti F, Sette G, et al. Identification and expansion of the tumorigenic lung cancer stem cell population. *Cell Death Differ* 2008;15:504–514.
19. Maemondo M, Inoue A, Kobayashi K, et al.; North-East Japan Study Group. Gefitinib or chemotherapy for non-small-cell lung cancer with mutated EGFR. *N Engl J Med* 2010;362:2380–2388.
20. Hirsch FR, Varella-Garcia M, McCoy J, et al.; Southwest Oncology Group. Increased epidermal growth factor receptor gene copy number detected by fluorescence in situ hybridization associates with increased sensitivity to gefitinib in patients with bronchioloalveolar carcinoma subtypes: a Southwest Oncology Group Study. *J Clin Oncol* 2005;23:6838–6845.
21. Cappuzzo F, Hirsch FR, Rossi E, et al. Epidermal growth factor receptor gene and protein and gefitinib sensitivity in non-small-cell lung cancer. *J Natl Cancer Inst* 2005;97:643–655.
22. Wang L, Schulz TC, Sherrer ES, et al. Self-renewal of human embryonic stem cells requires insulin-like growth factor-1 receptor and ERBB2 receptor signaling. *Blood* 2007;110:4111–4119.
23. Chen X, Levkowitz G, Tzahar E, et al. An immunological approach reveals biological differences between the two NDF/heregulin receptors, ErbB-3 and ErbB-4. *J Biol Chem* 1996;271:7620–7629.
24. Basak SK, Veena MS, Oh S, et al. The malignant pleural effusion as a model to investigate intratumoral heterogeneity in lung cancer. *PLoS ONE* 2009;4:e5884.
25. Mancini R, Giarnieri E, De Vitis C, et al. Spheres derived from lung adenocarcinoma pleural effusions: molecular characterization and tumor engraftment. *PLoS ONE* 2011;6:e21320.
26. Vescio RA, Connors KM, Youngkin T, et al. Cancer biology for individualized therapy: correlation of growth fraction index in native-state histoculture with tumor grade and stage. *Proc Natl Acad Sci USA* 1990;87:691–695.
27. Vescio RA, Connors KM, Bordin GM, et al. The distinction of small cell and non-small cell lung cancer by growth in native-state histoculture. *Cancer Res* 1990;50:6095–6099.
28. Yoshimasu T, Ohta F, Oura S, et al. Histoculture drug response assay for gefitinib in non-small-cell lung cancer. *Gen Thorac Cardiovasc Surg* 2009;57:138–143.
29. Pfragner R, Freshney RI. Culture of human tumor cells. *Wiley-Liss*; 2004:1–21.
30. Kobayashi H, Tanisaka K, Doi O, et al. An in vitro chemosensitivity test for solid human tumors using collagen gel droplet embedded cultures. *Int J Oncol* 1997;11:449–455.
31. Higashiyama M, Oda K, Okami J, et al. Prediction of chemotherapeutic effect on postoperative recurrence by in vitro anticancer drug sensitivity testing in non-small cell lung cancer patients. *Lung Cancer* 2010;68:472–477.
32. Ricci-Vitiani L, Lombardi DG, Pilozzi E, et al. Identification and expansion of human colon-cancer-initiating cells. *Nature* 2007;445:111–115.
33. Noro R, Gemma A, Kosaihira S, et al. Gefitinib (IRESSA) sensitive lung cancer cell lines show phosphorylation of Akt without ligand stimulation. *BMC Cancer* 2006;6:277.
34. Hynes NE, Lane HA. ERBB receptors and cancer: the complexity of targeted inhibitors. *Nat Rev Cancer* 2005;5:341–354.
35. Vermeer PD, Einwalter LA, Moninger TO, et al. Segregation of receptor and ligand regulates activation of epithelial growth factor receptor. *Nature* 2003;422:322–326.
36. Hinohara K, Kobayashi S, Kanauchi H, et al. ErbB receptor tyrosine kinase/NF-κB signaling controls mammosphere formation in human breast cancer. *Proc Natl Acad Sci USA* 2012;109:6584–6589.
37. Engelman JA, Jänne PA, Mermel C, et al. ErbB-3 mediates phosphoinositide 3-kinase activity in gefitinib-sensitive non-small cell lung cancer cell lines. *Proc Natl Acad Sci USA* 2005;102:3788–3793.
38. Sakai K, Yokote H, Murakami-Murofushi K, Tamura T, Saijo N, Nishio K. Pertuzumab, a novel HER dimerization inhibitor, inhibits the growth of human lung cancer cells mediated by the HER3 signaling pathway. *Cancer Sci* 2007;98:1498–1503.

FIGURE LEGENDS

FIGURE 1. Preparation and characterization of CTOSs from patients' lung tumors. *A*, H&E staining of original tumor and phase contrast images of organoid fraction at the indicated times after OMLC-58 preparation. Low- (upper panels) and high-magnification (lower panels) images are shown. Scale bar: 200 μm. *B*, Phase contrast images of CTOSs from three independent pleural effusion samples. Scale bar: 200 μm. *C*, Flow cytometric analysis of the indicated cell surface antigens by specific antibodies (solid line) or isotype controls (gray filled). *D*, OMLC-40 subjected to H&E staining and immunohistochemistry of E-cadherin (green), α-SMA (red), CD68 (red), and Hoechst33342 (blue). Scale bar: 75 μm.

FIGURE 2. CTOS-derived xenotumors preserved the original characteristics of parental tumors. *A*, H&E staining of the indicated cases. *B*, Immunohistochemistry of EGFR from the indicated cases. Original tumor (left column), CTOS (middle column), and xenograft tumor (right column). Adeno, adenocarcinoma; Squamous, squamous cell carcinoma; LCNEC, large-cell neuroendocrine carcinoma. Scale bar: 100 μm.

FIGURE 3. Effect of erlotinib on CTOS growth and signal transduction. *A*, In vitro dose-response curve of erlotinib sensitivity with 10 clinical cases. Origins of the cases are indicated in ascending order of IC50. *B*, Western blot of EGFR signaling pathway from 10 clinical cases, in ascending order of IC50. CTOSs were cultured under growth factor-starved conditions and pulsed for 15 min with 10 ng/mL EGF in the presence or absence of 1 μM erlotinib. *C*, Effects of erlotinib on the growth of xenograft tumors derived from OMLC-145 (EGFR overexpresser), OMLC-10 (EGFR-non expresser), OMLC-149 (EGFR wt), and OMLC-40 (EGFR wt). The CTOSs were transplanted in NOD/scid mice ($n = 5$). Erlotinib was administered po qd ×5 for two weeks, indicated as black bars. Tumor volume at each time point (V) was corrected by that on day 1 (V0). Open circles, vehicle-treated controls; closed circles, erlotinib-treated groups. $*p < 0.05$

FIGURE 4. Neuregulin1 stimulated CTOS growth in vitro. Growth ratio of CTOSs from six cases at day 7 relative to day 0. The CTOSs were embedded in Matrigel GFR and cultured in StemPro hESC or defined conditions containing neuregulin1 (NRG1), Long-IGF (IGF), bFGF, Activin A (Activin), or EGF at 10 ng/mL or 100 ng/mL. $*p < 0.05$.

FIGURE 5. Effect of NRG1 on pathway activation in CTOSs. *A*, Western blot for ErbB family signaling pathway of OMLC-128 and OMLC-53. CTOSs were cultured under growth factor-starved conditions and stimulated by 10 ng/mL of each indicated growth factor for 15 min. SP; StemPro hECS, NRG1; neuregulin1, IGF; Long-IGF1, Activin; Activin A. *B*, Immunohistochemistry of phospho-HER3 and phospho-AKT after NRG1 stimulation. OMLC-128 or OMLC-53 CTOSs were cultured under starvation conditions and stimulated by 10 ng/mL NRG1 for 6 h (pHER3) or 1 h (pAKT). EGFR, ZO1, and E-cadherin (CDH1) staining indicate the polarity of the CTOSs. *C*, Inhibitory effect of anti-HER3 antibody on growth of OMLC-128 CTOSs. CTOSs were embedded in Matrigel GFR, cultured in basal medium containing 10 ng/mL NRG1 or StemPro hESC, and treated with the indicated doses of anti-HER3 antibody. $*p < 0.05$. *D*, Effect of anti-HER3 antibody on signal transduction of OMLC-128. CTOSs were cultured in StemPro containing the indicated dose of anti-HER3 antibody for 24 h.

SUPPLEMENTARY FIGURE 1. *A*, Time-lapse analysis of CTOS formation from OMLC-145. Phase contrast images are shown. Scale bar: 100 μm. *B*, Phase contrast images of the organoid fraction (upper panel) and the flow-through fraction (lower panel) from OMLC-40 at day 1 after tumor dissociation. Arrow head indicates a

CTOS-like structure in the flow-through fraction. Scale bar: 100 μm. *C*, Flow cytometric analysis of Annexin-V and PI staining; CTOSs from OMLC-58 and OMLC-149 were dissociated into single cells, and cell death was analyzed at indicated time points.

SUPPLEMENTARY FIGURE 2. Immunohistochemistry for p53 (*A*), cytokeratin 7 (*B*), and NCAM (*C*) from indicated samples. Scale bar: 100 μm.

SUPPLEMENTARY FIGURE 3. Flow cytometric analysis of CD133 expression of CTOSs from three different patients. The tumor samples were digested and the cells and the fragments that passed through the 250-μm mesh filter were divided into two tubes. One was digested into single cells (bulk tumor). CTOS was prepared as described above from another tube and then digested into single cells. The cells were stained with the CD133 antibody (open area) or with an isotype control (grey area).

SUPPLEMENTARY FIGURE 4. Culture conditions of lung CTOSs. *A*, Effect of extracellular matrix and medium on CTOS growth. Growth ratio is the relative CTOS size at day 7 to that on day 0. The CTOSs were cultured in suspension (Sus), in Cell

Matrix type IA (CM), or in Matrigel GFR (MG). Gray bars, StemPro medium; black bars, DMEM with 10% serum. *B*, Growth ratio of CTOS from adenocarcinoma (OP Ad) or squamous cell carcinoma (OP Sq) from surgical specimen, or adenocarcinoma from pleural effusion (Pleural Ad). CTOSs were embedded in Matrigel GFR and cultured in StemPro hESC for 7 days. Each dot represents the average growth of each sample.

SUPPLEMENTARY FIGURE 5. *A*, Immunoblot of EGFR from six clinical cases. Immunoblot of β-actin is shown as a loading control. *B*, Image of DNA FISH analysis. Orange signal indicates EGFR, and green signal indicates the chromosome 7 centromere region. Inlet numbers are average values of EGFR gene amplification. *C*, Western blotting of the molecules on the EGFR signaling pathway from OMLC-149 (EGFR wt). CTOSs were cultured under starvation conditions and pulsed for 15 min with 10 ng/mL EGF in the presence or absence of 1 μM erlotinib or 1 μM gefitinib. *D*, Dose-response curve of gefitinib with OMLC-149.

SUPPLEMENTARY MATERIALS AND METHODS

FACS Analysis

Cells in CTOSs were dissociated into single cells by 0.05% trypsin-EDTA, and filtered through a 40-μm cell strainer. Cells were stained with FITC anti-human EpCAM (Miltenyi), PE anti-human CD45 (BD Pharmingen), or PE anti-CD133 (Miltenyi), according to the manufacturer's instructions. For apoptosis detection, the cells were cultured in StemPro hESC for the indicated time, and labeled with Annexin V and propidium iodide (PI) using the Annexin V-FITC Apoptosis Detection Kit (Biovision). Flow cytometry was performed with a FACSCalibur (Becton-Dickinson, Franklin Lakes, NJ) and analyzed using FlowJo software (Tree Star, Inc., Ashland, OR).

Immunohistochemistry

Primary antibodies used were E-cadherin (clone36/E-cadherin, BD), α-SMA (cloneIA4, SIGMA), CD68 (cloneKP1, DAKO), EGFR (cloneD38B1, CST), cytokeratin 7 (cloneOV-TL12/30, DAKO), p53 (cloneDO-7, Novocastra), NCAM (AG1, DSHB), pAKT (Ser473) (clone D9E, CST), pHER3 (Y1289) (clone21D3, CST), and Zo-1 (Invitrogen).

Western Blotting

Primary antibodies against pEGFR (Tyr1068, cloneD7A5), EGFR (clone D38B1), pHER2 (Y1221/1222, clone6B12), pHER3 (Y1289, clone21D3), pAKT (Ser473, cloneD9E), AKT (clone40D4), pERK1/2 (Thr202/Tyr204, cloneD13.14.4E), and ERK1/2 (clone3A7) were obtained from Cell Signaling Technology; HER2 (A0485) from DAKO; HER3 (clone5A12) from NanoTools; and β-actin (cloneAC-15) from SIGMA.

SUPPLEMENTARY FIGURE 1

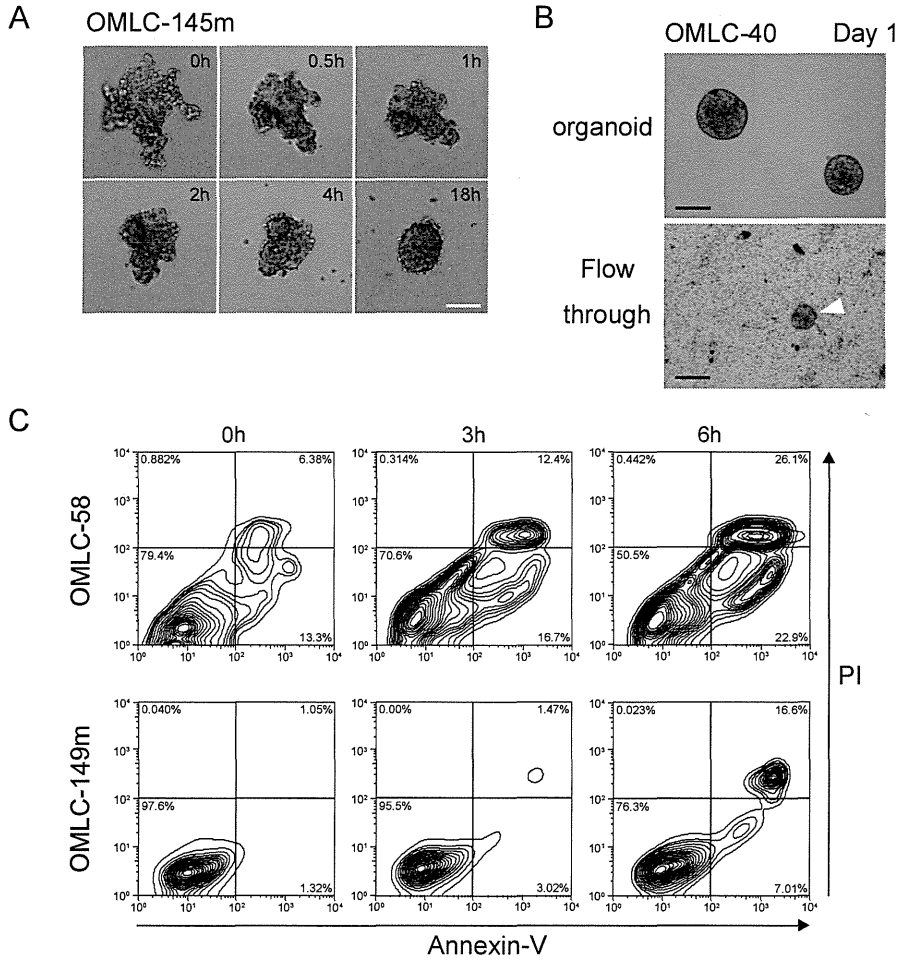

SUPPLEMENTARY FIGURE 2

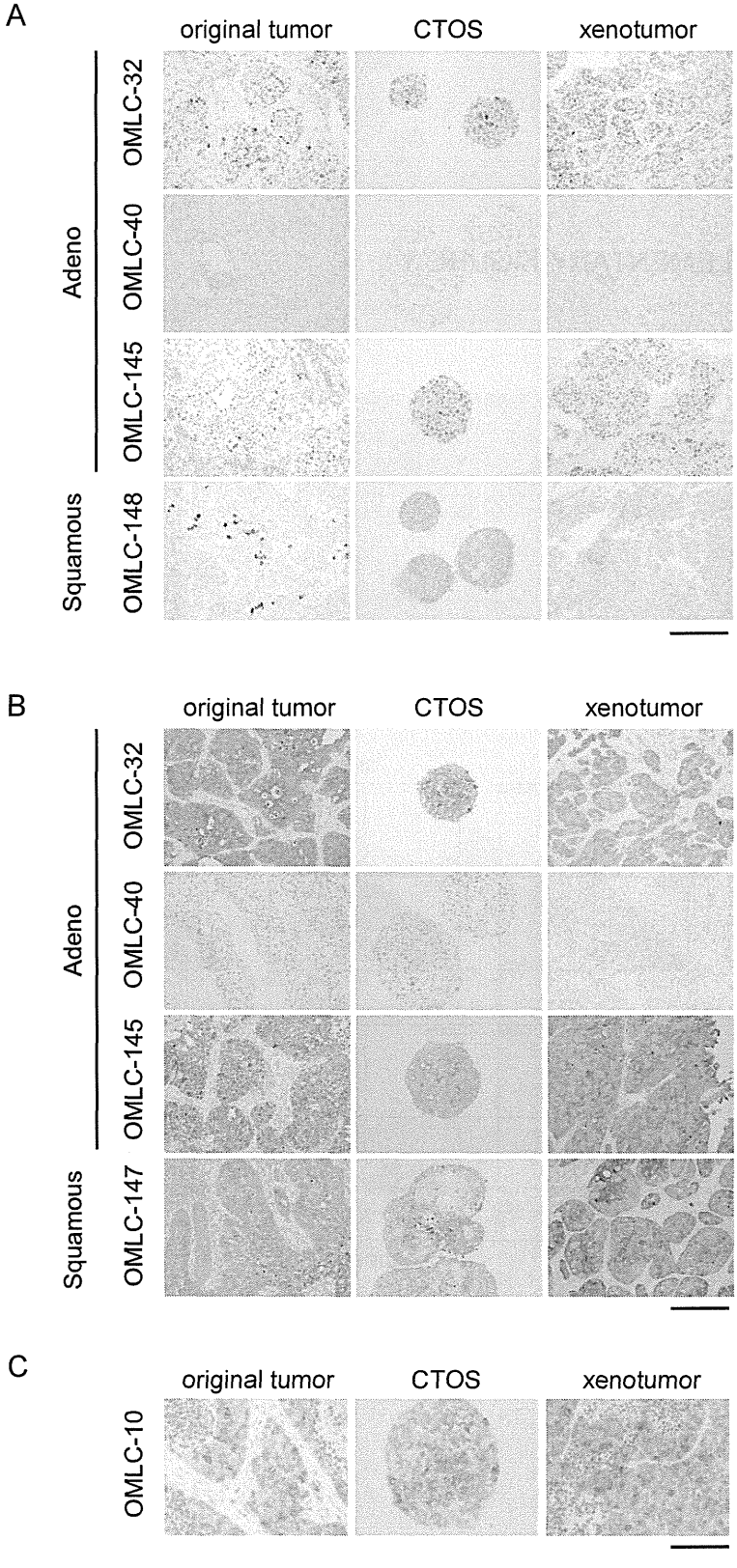

SUPPLEMENTARY FIGURE 3

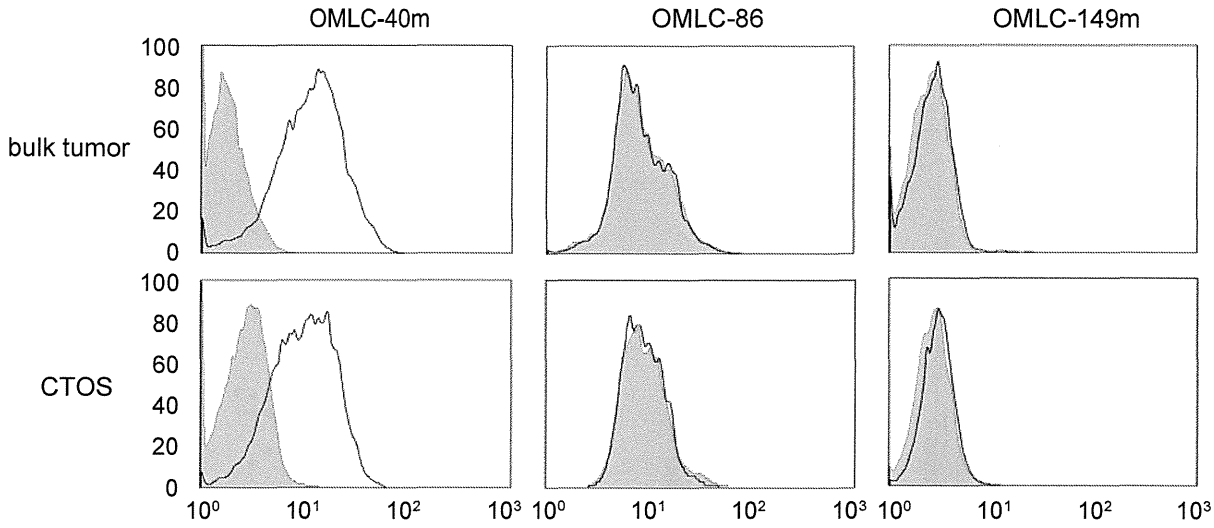

SUPPLEMENTARY FIGURE 4

A

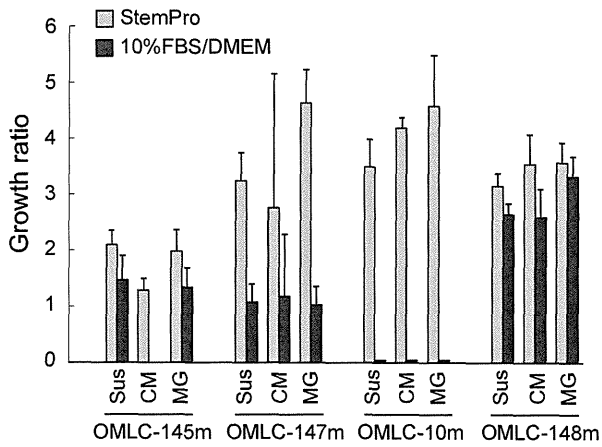

B

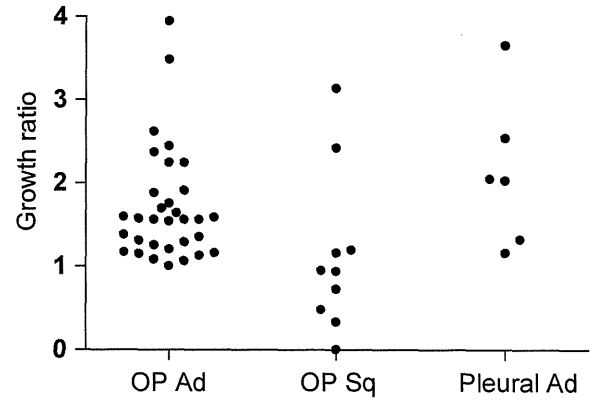

SUPPLEMENTARY FIGURE 5

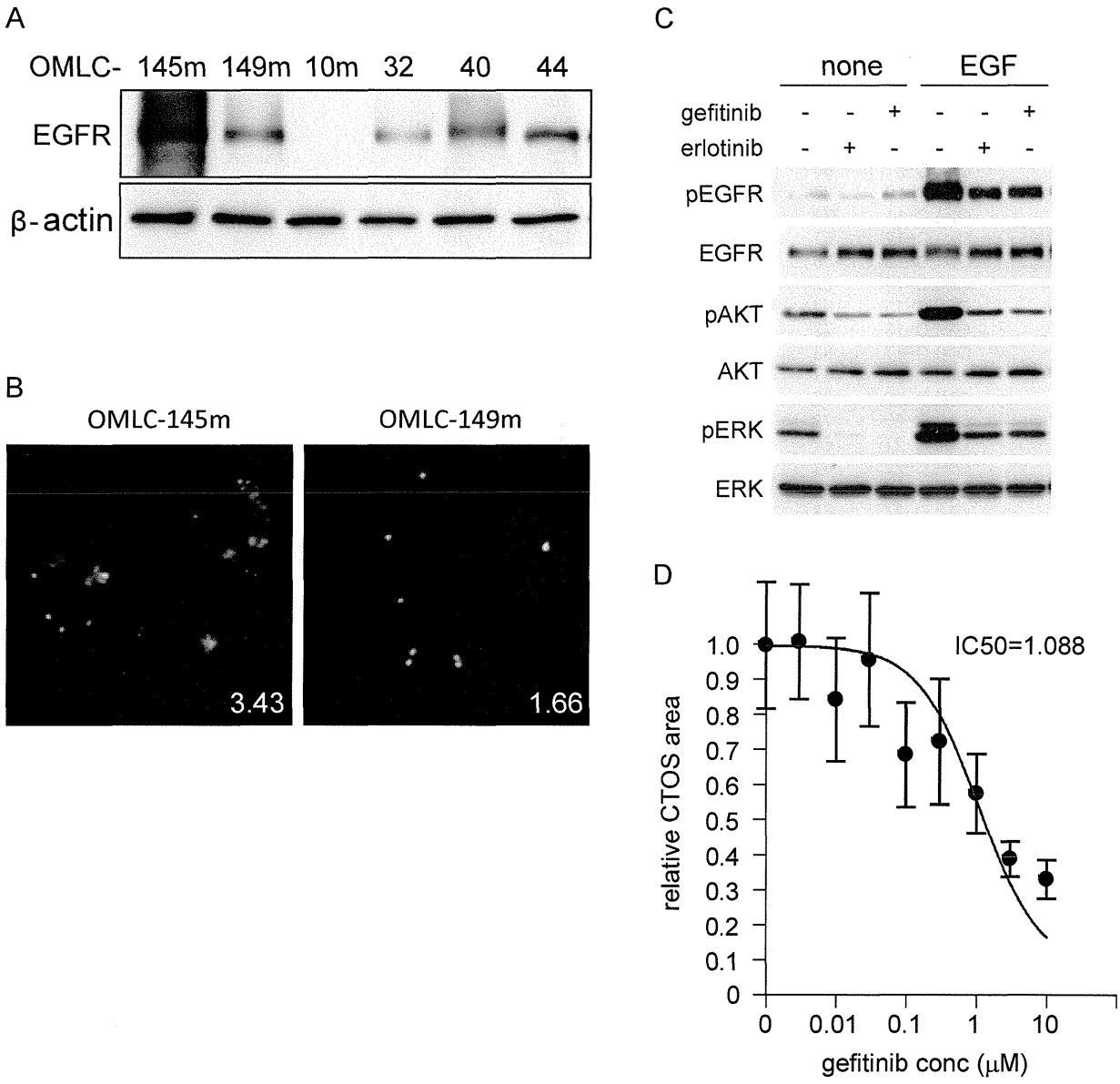

SPPLEMENTARY TABLE 1 Case descriptions and CTOS formation from lung cancer patients

	ID	Age	Sex	Histology	Stage	CTOS formation	EGFR gene mutation	Xenogfaft formation	NRG1-induced growth
Surgical sample	OMLC-1	80	M	Ad	IB	yes			
	OMLC-2	68	M	Sq	IA	yes			
	OMLC-3	48	M	Large	IIIA	yes			
	OMLC-4	69	F	Ad	IB	yes			
	OMLC-5	74	M	LCNEC	IIB	yes		no	
	OMLC-6	70	M	Sq	IB	yes			
	OMLC-7	59	M	Ad	IIB	yes			
	OMLC-8	75	M	small	IB	yes			
	OMLC-9	80	F	Ad	IB	yes		no	
	OMLC-10	77	M	LCNEC	IB	yes		yes	
	OMLC-11	39	F	Ad	IIIA	yes		no	
	OMLC-12	67	F	Ad	IIIB	yes			
	OMLC-13	56	F	Ad	IB	yes			
	OMLC-14	56	M	Sq	IB	yes			
	OMLC-15	67	M	Ad	IV	no			
	OMLC-16	73	F	Ad	IIA	yes			
	OMLC-17	53	F	Ad	IIIB	no			
	OMLC-18	67	M	Ad	IIIB	no			
	OMLC-19	76	F	Ad	IB	no			
	OMLC-20	78	F	Ad	IB	no			
	OMLC-21	67	M	Ad	IB	yes			
	OMLC-22	67	M	LCNEC	IB	yes			
	OMLC-23	53	F	Ad	IIIA	yes			
	OMLC-24	68	M	small	IA	yes			
	OMLC-25	67	M	Ad	IA	yes			
	OMLC-26	70	F	Ad	2B	yes			
	OMLC-27	68	F	Ad	IB	yes			
	OMLC-28	68	F	Sq	IIA	yes			
	OMLC-29	60	M	Ad	IIB	yes			
	OMLC-30	59	M	AdSq	IIIB	yes			
	OMLC-31	65	F	AdSq	IIB	yes			
	OMLC-32	72	M	Ad	IB	yes		yes	
	OMLC-33	61	M	Ad	IIIA	no		no	
	OMLC-34	76	M	Sq	IB	yes		no	
	OMLC-35	62	M	Sq	IA	yes			
	OMLC-36	61	M	pleomorphic	IIB	no			
	OMLC-37	66	M	AdSq	IA	yes			
	OMLC-38	83	M	Ad	IIIA	yes		no	
	OMLC-39	61	M	Sq	IB	yes			
	OMLC-40	60	F	Ad	IIB	yes		yes	
	OMLC-41	60	F	pleomorphic	IIB	yes			
	OMLC-42	73	F	Ad	IA	no			
	OMLC-43	61	F	Ad	IB	no			
	OMLC-44	75	F	Ad	IV	yes	L858R		
	OMLC-45	81	M	Ad	IIB	yes		no	
	OMLC-46	77	M	Ad	IA	yes		no	
	OMLC-47	68	M	Sq	IB	yes			
	OMLC-48	80	M	Ad		yes			
	OMLC-49	85	F	Ad	IB	yes			
	OMLC-50	47	M	Ad	IIIA	yes			
	OMLC-51	69	F	Ad	IB	yes			
	OMLC-52	59	M	Ad		yes			
	OMLC-53	70	F	Ad	IB	yes	G719C	no	yes
	OMLC-54	68	M	Sq	IB	yes			
	OMLC-55	82	M	Sq	IA	yes			
	OMLC-56	61	F	Ad	IA	yes			
	OMLC-57	73	M	Sq	IIIA	yes			
	OMLC-58	67	M	AdSq	IIA	yes			
	OMLC-59	81	M	Ad	IA	no			
	OMLC-60	81	F	Ad	IB	yes			
	OMLC-61	63	F	Sq	IIB	yes			
	OMLC-62	59	M	Ad	IV	no			
	OMLC-63	74	M	Sq	IV	no			
	OMLC-64	78	M	Ad	IA	yes			
	OMLC-65	60	M	Ad	IA	yes	L858R		

	ID	Age	Sex	Histology	Stage	CTOS formation	EGFR gene mutation	Xenogfaft formation	NRG1-induced growth
	OMLC-66	65	F	Ad	IB	no			
	OMLC-67	75	M	Sq	IIIA	no			
	OMLC-68	61	M	Ad	IA	yes			
	OMLC-69	77	F	Sq	IA	yes			
	OMLC-70	71	M	Ad	IIIA	yes			
	OMLC-71	75	M	Sq	IB	yes			
	OMLC-72	55	M	Ad	IB	yes			
	OMLC-73	60	M	Ad	IB	yes			
	OMLC-74	64	F	Ad	IB	yes			
	OMLC-75	55	F	Ad	IIB	yes			
	OMLC-76	46	F	Ad	IIIA	yes			
	OMLC-77	71	F	Ad	IB	no			
	OMLC-78	55	M	Ad	IIB	no			
	OMLC-79	69	F	Sq	IA	no			
	OMLC-80	54	M	Ad	IB	yes			
	OMLC-81	73	M	Ad	IA	yes			
	OMLC-82	71	M	Ad	IA	yes			
	OMLC-83	57	M	Ad	IA	yes			
	OMLC-84	76	M	Sq	IA	yes			
	OMLC-85	60	M	Sq	IB	no			
	OMLC-86	74	F	Ad	IIIA	yes			
	OMLC-87	59	F	Ad	IB	no			
	OMLC-88	71	F	Sq	IB	yes			
	OMLC-89	61	M	Ad	IB	yes			
	OMLC-90	65	F	Ad	IA	no			
	OMLC-91	75	M	Sq	IA	yes			
	OMLC-92	56	F	Ad	IB	yes			
	OMLC-93	62	M	Ad	IV	yes			
	OMLC-94	73	F	Sq	IIA	yes			
	OMLC-95	61	M	Sq	IIIA	yes			
	OMLC-96	45	F	Ad	IB	yes			
	OMLC-97	68	M	Sq	IIIB	yes			
	OMLC-98	70	M	Sq	IA	yes			
	OMLC-99	55	M	Ad	IIIA	yes		yes	
	OMLC-100	68	M	Sq	IIA	yes			
	OMLC-101	83	F	Ad	IB	yes			
	OMLC-102	70	M	Ad	IIA	yes			
	OMLC-103	46	F	Ad	IA	yes			
	OMLC-104	65	M	Ad	IA	yes			
	OMLC-105	46	M	Ad	IIIA	no			
	OMLC-106	68	M	Sq	IIA	yes			
	OMLC-107	61	M	AdSq	IIB	yes			
	OMLC-108	64	M	Ad	IIIA	yes			
	OMLC-109	65	F	Ad	IIIA	yes			
	OMLC-110	70	M	Sq	IB	yes			
	OMLC-111	74	F	Ad	IA	yes			
	OMLC-112	64	F	Ad	IV	yes			
	OMLC-113	82	M	AdSq	IB	yes			
	OMLC-114	50	M	Sq	IIB	no			
	OMLC-115	77	F	Ad	IIA	yes			
	OMLC-116	69	F	Ad	IA	no			
	OMLC-117	65	M	Sq	IB	yes			
	OMLC-118	76	F	Ad	IB	yes			
	OMLC-119	81	F	Ad	IB	yes			
	OMLC-120	73	F	Ad	IB	no			
	OMLC-121	63	F	Ad	IIIA	yes			
	OMLC-122	70	M	Ad	IB	yes			
	OMLC-123	65	F	Ad	IIB	yes			
	OMLC-124	61	M	Ad	IA	yes	wt		yes
	OMLC-125	69	F	Ad		yes			
	OMLC-126	59	M	Ad	IA	yes			yes
Pleural effusion	OMLC-127	65	M	Ad	IV	yes	wt		yes
	OMLC-128	63	M	Ad	IV	yes	ex19 del/ T790M	no	yes
	OMLC-129	64	M	Ad	IV	no			
	OMLC-130	67	M	Ad	IV	no			
	OMLC-131	70	M	Ad	IV	no			
	OMLC-132	55	M	Ad	IV	no			

	ID	Age	Sex	Histology	Stage	CTOS formation	EGFR gene mutation	Xenogfaft formation	NRG1-induced growth
	OMLC-133	58	M	Sq	Ⅳ	no			
	OMLC-134	63	M	Ad	Ⅳ	yes	wt	yes	yes
	OMLC-135	53	M	Ad	Ⅳ	no			
	OMLC-136	56	M	Ad	Ⅳ	no			
	OMLC-137	71	F	Ad	Ⅳ	yes			
	OMLC-138	66	M	AdSq	Ⅳ	yes	L858R	yes	yes
	OMLC-139	62	M	Ad	Ⅳ	yes	wt	no	no
	OMLC-140	72	F	Ad	Ⅳ	no			
	OMLC-141	73	M	Sq	Ⅳ	no			
	OMLC-142	37	M	Ad	Ⅳ	yes	ex19 del		yes
	OMLC-143	68	F	Ad	Ⅳ	yes			
	OMLC-144	73	M	Ad	Ⅳ	no			
Mouse xenograft	OMLC-145	65	M	Ad	Ⅳ	yes	gene amp.	yes	yes
	OMLC-146	74	M	Sq	ⅠB	yes		no	
	OMLC-147	73	M	Sq	ⅠB	yes		yes	no
	OMLC-148	64	F	Sq LNmet	ⅢA	yes		yes	no
	OMLC-149	57	F	Ad	ⅡA	yes	wt	yes	yes

Ad: adenocarcinoma, Sq: squamous cell carcinoma, AdSq: adenosquamouse cell carcinoma,
Small: small cell carcinoma, Large: large cell carcinoma
LCNEC: large cell neuroendocrine carcinoma, Pleomorphic: pleomorphic carcinoma,
LNmet: lymphnode metastasis, blank: not assessed.